Ecology

Article

Nonlinear effects of temperature on mosquito parasite infection across a large geographic climate gradient

Johannah E. Farner[1*], Kelsey P. Lyberger[2], Lisa I. Couper[3], Mauricio Cruz-Loya[1], Erin A. Mordecai[1]

[1]Department of Biology, Stanford University, Stanford, CA 94305, USA; [2] College of Integrative Sciences and Arts, Arizona State University, Mesa, AZ 85212, USA; [3] Division of Environmental Health Sciences, University of California, Berkeley, Berkeley, CA 94720, USA.

*Corresponding author: jfarner@stanford.edu

Upon acceptance, data and code will be provided via Dryad.

Key words/phrases: *Aedes sierrensis;* disease ecology, *Lambornella clarki*; parasitism; thermal biology thermal performance curve

Abstract

Temperature drives ectothermic host – parasite interactions, making them particularly sensitive to climatic variation and change. To isolate the role of temperature, lab-based studies are increasingly used to assess and forecast disease risk under current and future climate conditions. However, in the field, the effects of temperature on parasitism may be mediated by other sources of variation, including local adaptation of hosts and parasites to one another and to the environment. To address the key knowledge gaps of how temperature influences host – parasite interactions and whether thermal responses measured in controlled experiments capture infection across temperature gradients in nature, we paired an extensive field survey of parasitism—by the ciliate *Lambornella clarki* on its tree hole mosquito host, *Aedes sierrensis*—with laboratory experiments describing parasitism thermal performance curves (TPCs) for six host populations from varying climates. We also investigated the mechanisms underlying the thermal biology of the host – parasite interaction by separately measuring TPCs for infection, host immunity, and parasite growth rates. Along the west coast of North America, across an 1100 km climate gradient spanning 12ºC mean rainy season temperature variation, we found that parasitism peaked at intermediately cold temperatures of 9.2 – 10ºC, and was consistent both between field seasons and with the lab experiment results. In the laboratory experiments, infection thermal responses were consistently nonlinear and peaked at 8.4 – 10ºC, showing no evidence of host intraspecific variation in temperature sensitivity to parasitism. Importantly, parasitism peaked at temperatures below the thermal optimum for free-living *L. clarki* due to the balance of temperature effects on parasite growth and reproduction against the strength of the host melanization immune response. The results suggest that nonlinear responses to temperature

drive parasitism in nature, and that simple lab and field studies can accurately capture the thermal biology of multilayered host – parasite interactions.

Introduction

Climate warming is fundamentally important to infectious disease risk because temperature drives many of the constituent biological processes of host – parasite interactions, including host and parasite growth and development, contact rates, and immune functions (Kutz et al., 2005; Labaude et al., 2017; Laughton et al., 2017; Franke et al., 2019; Mordecai et al., 2019). Strong relationships between temperature and parasitism are frequently observed in laboratory experiments and captured in thermal performance curves (TPCs) that quantify how infection rates change with temperature, typically from data collected across a range of constant incubation temperatures (Angilletta 2009; Gehman et al., 2018; Kirk et al. 2018; Padfield et al., 2020). Following expectations from biochemical first principles, TPCs are commonly unimodal, with biological rates increasing with temperature from their critical thermal minimum, peaking at a thermal optimum, and then declining up to a critical thermal minimum (Angilletta, 2009). Researchers increasingly use TPCs to assess nonlinear shifts in disease risk based on current and forecasted climate and weather conditions (Gehman et al., 2018; Ryan et al., 2019; Aleuy et al., 2023). However, it is unclear whether TPCs measured in controlled laboratory settings fully capture the thermal response of disease in natural settings, where environmental complexity may modify or outweigh parasitism - temperature relationships (Mordecai et al., 2019; Taylor et al., 2019).

Parasitism TPCs are typically measured for single laboratory populations, in the absence of other stressors, and are infrequently compared to disease burdens along temperature gradients in the field (e.g., Gehman et al., 2018; Mordecai et al., 2019; Padfield et al., 2020). Although an

increasing number of studies describe thermal responses for multiple populations or genotypes within host-parasite systems (Mazé-Guilmo et al., 2016; Ahrens et al., 2019; Franke et al., 2019; Aleuy et al., 2023; Ragonese et al., 2024), research on statistical or correlative relationships between TPCs for disease transmissibility (e.g., R_0) and natural infection patterns has thus far relied on laboratory measurements from single host and parasite populations or clones, and field data collated from disparate sources and/or collected over small geographic areas. To date, this research has focused primarily on mosquito-borne human disease and fungal pathogens of zooplankton (Mordecai et al., 2013; 2017; Shocket, Ryan et al., 2018; Shocket, Strauss et al., 2018; Tesla et al., 2018; Shah et al., 2019; Shocket et al., 2020; Kirk et al., 2024). However, TPCs for both hosts and parasites can vary geographically within species due to local adaptation and population structure (Sinclair et al., 2012; Gaitán-Espitia et al., 2014; Mazé-Guilmo et al., 2016; Jurriaans & Hoogenboom, 2019; Aleuy et al., 2023; Couper et al., 2024), and additional environmental variability in field settings may outweigh or modify the temperature dependence of parasitism (e.g., Boots, 2000; Seppälä et al., 2008; Hall et al., 2009; Penczykowski et al., 2014; Palmer-Young et al., 2019; Brown et al., 2023). Thus, there is a critical need to address the questions of how temperature affects parasitism in the field, whether lab-based TPC estimates can accurately, and mechanistically, capture these patterns, and whether local thermal adaptation modifies the temperature-dependence of parasitism.

Central to capturing the thermal biology of parasitism is understanding the host and parasite mechanisms that drive the interaction. For example, host life history and defense traits and parasite growth, attack, dispersal, and transmission traits may each respond nonlinearly and distinctly to temperature. The combined effect of these traits determines the overall impact of temperature on parasitism (Paull et al., 2012; Shocket et al., 2018; Mordecai et al., 2019; Sun et

al., 2023). Moreover, host and parasite trait thermal responses may differ across populations due to local adaptation and across environmental conditions (Thomas & Blanford, 2003; Sternberg & Thomas, 2014). Given that it is not feasible to measure TPCs for every possible combination of host population, parasite population, and environmental context, it is important to establish whether TPCs measured for a single set of populations and conditions can generalize to cover entire species ranges, and which traits capture the essential thermal biology of the interaction. Here, we address these questions in a model system of a mosquito (*Aedes sierrensis*) and its facultative ciliate parasite (*Lambornella clarki*), which occur across a large geographic gradient in western North America.

In this study, we pair field surveys along the entire west coast of the continental United States—spanning the geographic range of the host species—with laboratory experiments describing the temperature dependence of infection and key traits involved in host defenses and parasite fitness, for host populations from different climates across the survey area. Both species are short-lived ectotherms that are directly affected by environmental temperatures, occur commonly across a large geographic climate gradient in discrete tree hole habitats that are naturally replicated across landscapes, and can be reared separately and together in the lab (Washburn & Anderson, 1986; Broberg & Bradshaw, 1997; Darsie & Ward, 2005; Ismail et al., 2023; Lyberger et al., 2024). A 1986 field survey found that infection occurrence increased from southern to northern California (Washburn & Anderson, 1986). Our recent work describing temperature effects on different populations of *Ae. sierrensis, L. clarki*, and their interactions indicates that infection has a consistent nonlinear relationship with temperature for both sympatric and allopatric pairs of host and parasite populations collected across climates, despite evidence of local thermal adaptation in free-living *L. clarki* populations (Ismail et al., 2023;

Lyberger et al., 2024). This body of work generates the hypothesis that parasitism responds to temperature as a function of the thermal biology of multiple host and parasite traits. However, it is unknown whether the lab-measured temperature impacts on parasitism across different *Ae. sierrensis* host populations are borne out in infection occurrence across the environmentally complex species range.

Methods

Study system

Ae. sierrensis and its facultative ciliate parasite *L. clarki* occur across western North America in seasonally rainwater-filled tree holes, where mosquitoes undergo one reproductive cycle annually in which larvae feed on detritus and microbes (including free-living *L. clarki*) before pupating and emerging as adults, and free-living *L. clarki* ciliates feed on aquatic bacteria (Washburn & Anderson, 1986; Darsie & Ward, 2005). In the presence of *Ae. sierrensis* larvae, free-living *L. clarki* irreversibly transform into parasites that attack larval mosquitoes by attaching to the larval cuticle, penetrating into the body cavity, and then replicating, often to high densities that kill hosts after a few weeks (Washburn et al., 1988). Mosquitoes can resist infection through multiple defenses that each likely respond nonlinearly to temperature: melanization (a generalized immune response), molting between larval instars, developing into pupae, and consuming free-living *L. clarki* in the water column (Clark & Brandl, 1976; Washburn et al., 1988; Washburn et al., 1991; Suwanchaichinda & Paskewitz, 1998; Christensen et al., 2005; Murdock et al., 2012; Martin & Hillyer, 2024). Beyond the previously documented latitudinal gradient, *L. clarki* presence is not correlated with habitat characteristics such as tree hole size, exposure, height above ground, or tree species (Washburn & Anderson, 1986).

Field survey

To document infection patterns over a large geographic temperature gradient and collect materials for lab experiments, we sampled from over 500 water-filled tree hole habitats containing *Ae. sierrensis* larvae spanning 1100 km north to south with a mean November – April rainy season temperature gradient of 2.6ºC to 15.3ºC in California, Oregon, and Washington, USA, during the rainy seasons of 2022 and 2023 (Figure 1) (PRISM Climate Group, 2021). Each year, we started in the warmest and ended in the coolest locations to track the seasonal timing of *Ae. sierrensis* egg hatching and development (Jordan & Bradshaw, 1978; Jordan, 1980a; 1980b), collecting larval samples and examining them for infection at 10-40x magnification (Appendix S1). We aimed to sample each tree hole in both years, but had to replace some locations in 2023 due to storm damage (Figure 1).

For each sampling site, we used PRISM climate data to characterize long-term mean temperature conditions in the November – April rainy season when mosquito larvae and parasites are active in tree holes (PRISM Climate Group, 2021; Washburn & Anderson, 1986; Luković et al., 2021; Praskievicz & Chang, 2009). We chose the PRISM dataset for its long-term coverage of the entire study region. To assess the match between the remotely sensed PRISM data and the conditions in surveyed tree hole habitats, we placed iButton temperature loggers (Maxim Integrated, San Jose, CA, USA) in 84 arbitrarily selected tree holes across the survey area during the 2022 field season. These iButtons were retrieved the next year, and temperature logs were compared to PRISM estimates for the same locations during the intervening time period and found to be strongly correlated (R^2 mean = 0.94, SD = 0.03). Finally, we accessed NOAA climate reports that compared regional temperatures and precipitation in each field season to

159 long-term averages (NOAA National Centers for Environmental Information, 2022; 2023).
160 Additional details on the field survey methods are provided in Appendix S1.
161
162 *Lab experiments*
163 *1. Temperature-dependent infection experiment*
164 In September 2022, we measured the effects of temperature on the host – parasite interaction
165 with an experiment that used the F1 offspring of six host populations reared in the lab from
166 larvae collected in the 2022 field survey: two populations each from warm (14.8 – 15.1ºC rainy
167 season mean temperature; San Juan Capistrano and Trabuco Canyon, CA), intermediate (10.8 –
168 11.8ºC; Big Sur and Woodside, CA), and cool (5.3 – 6.5ºC; Shaver Lake, CA and Eugene, OR)
169 climates (Figure 1, Appendix S2: Table S1). We exposed each host population to the same
170 allopatric parasite culture isolated from an infected larva collected in Marin County, CA (10.6ºC)
171 (Figure 1), so that any variation observed in the temperature dependence of infection would be
172 due to the host population. Mosquito rearing and ciliate culturing occurred at 21.5ºC following
173 Ismail et al. (2023), Couper et al. (2024), and Lyberger et al. (2024).
174 For the experiment, mosquito eggs were hatched and day-old larvae were incubated in groups
175 of five with 7 mL parasite culture diluted to a standardized density of 35 ciliates per 100 uL at six
176 constant temperatures: 7ºC, 11ºC, 14ºC, 18ºC, 23ºC, and 28ºC (N = 6 microcosms per host
177 population per temperature, except for Big Sur, where N = 4 due to lower egg hatching, totaling
178 34 microcosms per temperature, and 204 microcosms overall). We monitored the proportions of
179 hosts with infections and parasite melanization spots, the survival of infected and uninfected
180 hosts, and *L. clarki* cell density per 100 uL liquid up to the first pupation at each temperature.
181 Because *Ae. sierrensis* development speed is thermally sensitive, we set monitoring frequences

182 that ensured at least four checkpoints spanning the host's four larval instars at each temperature;
183 these ranged from every two days at 28ºC to every seven days at 7ºC and 11ºC (Appendix S2:
184 Table S2).

185 2. *Host and parasite thermal responses in isolation*

186 To compare the thermal performance of mosquito larvae and ciliates to that of parasitism, we
187 incubated mosquito-only and ciliate-only microcosms alongside the infection experiment,
188 following the same design as above. The mosquito-only microcosms were monitored on the
189 same timeline as the infection experiment. For the ciliate-only microcosms (N = 6 wells per
190 temperature, 36 total microcosms), we measured the population growth rate by inoculating wells
191 with culture diluted to 4 cells per 100 uL and then counting the cells per 300 uL daily for four
192 days of positive growth.

193 To assess the temperature sensitivity of the host melanization process (removing the
194 temperature sensitivity of parasite attack rates), we performed a mechanical melanization assay
195 on fourth instar larvae from one population at 4, 8, 12, 16, 20, 24, and 28ºC (N = 6 wells of 5
196 mosquitoes per temperature with no ciliates, for 42 total microcosms). Additional details are
197 provided in Appendix S1.

198 *Statistical analyses*

199 *Field survey*

200 To investigate the nonlinear temperature dependence of parasitism, we tested for a quadratic
201 relationship between temperature and the presence of *L. clarki* infections in the surveyed tree
202 holes using a binomial generalized linear mixed effects model, with mean temperature, mean
203 temperature squared (to account for hypothesized nonlinear effects of temperature), and year as
204 fixed effects, and tree hole ID as a random effect. We used the glmer function in the R package

205 “lme4” with scaled and centered environmental variables, and assessed model fit with the R
206 package “DHARMa” (Bates et al., 2003; Hartig, 2017). Because interactions between survey
207 year and the temperature variables were not significant, we estimated the overall mean
208 temperature where infection was most likely to occur with a model that did not include year. We
209 additionally used general linearized models fit individually to the data from each survey year to
210 describe the temperatures where infection occurrence peaked within each field season. To
211 evaluate the relationship between within-tree hole habitat temperatures logged by iButtons and
212 the PRISM air temperature dataset used in the model, we tested for correlations, calculated the
213 mean differences between daily mean temperature time series recorded by iButtons and extracted
214 from PRISM, and used linear regression with the mean temperature recorded within a tree hole
215 as the dependent variable and the mean PRISM temperature estimate for that location as the
216 independent variable. Because there were only two field seasons, the NOAA annual climate
217 reports for each field season were not included in statistical analyses, but used only to
218 qualitatively compare the two years.

219 *Lab experiments*

220 To quantify the thermal sensitivity of the host – parasite interaction measured from the
221 laboratory experiment, we used a Bayesian approach to fit TPCs for the proportion of infected
222 hosts, the proportion of hosts with melanization spots, and the proportion of hosts killed by
223 infections. The total number of infections observed in each microcosm over the course of the
224 experiment depended on both initial parasite attack success and subsequent rounds of parasite
225 transmission following infected host deaths that released new parasites as killed mosquitoes
226 decomposed. We fit separate TPCs for both initial infection for the period up to the first deaths of
227 infected hosts at each temperature, when all observed infections resulted from the first round of

host – parasite interactions (covering checkpoints 1-3, approximately corresponding to larval instars 1-3), and total infection rates over the entire experiment (including all host-parasite interaction cycles for all four larval instars); we used the same procedure to fit initial and total TPCs for the proportions of hosts melanizing attacking parasites. We additionally fit TPCs for free-living *L. clarki* population growth rate and for the host melanization immune response induced by mechanical penetration of the cuticle. We planned to fit TPCs for host survival in the absence of parasitism, but >99% of larvae incubated without parasites survived across all temperatures. Because initial parasite success is likely to determine whether there is a non-zero infection probability over the rest of the season (Washburn et al., 1991), this is the laboratory-based TPC that we expect to most closely align with the field-observed response of infection occurrence to temperature.

Unimodal traits were fit with a flexTPC functional form (Equation 1) which can describe unimodal TPCs of any skewness (Cruz-Loya et al., *preprint*). Using this flexible function to fit TPCs of different shapes across our traits of interest allowed for ease of comparison of thermal responses among traits and populations.

$$r(T) = \begin{cases} r_{max}\left[\left(\frac{T - T_{min}}{\alpha}\right)^{\alpha}\left(\frac{T_{max} - T}{1-\alpha}\right)^{1-\alpha}\left(\frac{1}{T_{max} - T_{min}}\right)\right]^{\frac{\alpha(1-\alpha)}{\beta^2}} & T_{min} < T < T_{max} \\ 0 & \text{otherwise} \end{cases} \quad (1)$$

In this equation, T_{min} and T_{max} correspond to the minimum and maximum temperature, respectively, r_{max} to the maximum trait value, and α and β are parameters that determine the curve skewness and rate of decrease from the maximum trait value, respectively (Appendix S1). Host melanization increased monotonically with temperature, and was fit to a 4-parameter shifted logistic model (Equation 2, see Appendix S1 for derivation).

$$m(T) = \begin{cases} \dfrac{1}{\left[1 + (2^{1/s} - 1)\left(\dfrac{T_{50} - T_{min}}{T - T_{min}}\right)^{a}\right]^{s}} & T > T_{min} \\ 0 & \text{otherwise} \end{cases} \quad (2)$$

where T_{min} is the minimum temperature, T_{50} is the temperature at which 50% of the population is melanized, and a and s are constants that allow for different rates of change of melanization near T_{50} and for the response to be asymmetric, which was necessary to fit the data.

We used a binomial likelihood for all traits that were measured as proportions. For the free-living parasite population growth rate TPC, we used a Gamma likelihood with population growth rates obtained from the raw time-course data with the R package "growthrates" (Petzoldt, 2022). Optimal temperatures were calculated analytically using the posterior samples of the model parameters (Appendix S1). Details on model fitting and diagnostics are provided in Appendix S1.

To assess population variation in lab-measured thermal performance among host populations and the responses measured in the infection experiment, we compared 95% credible intervals for the thermal optimum (T_{opt}), maximum (T_{max}), and minimum (T_{min}) and interpreted non-overlapping intervals as evidence of biologically significant variation. We additionally compared the magnitudes of the 95% credible intervals over TPC plots for each population. Since the credible intervals for T_{opt}, T_{min}, and T_{max} overlapped for all populations for all measured traits, we combined the data to generate species-representative TPCs, which we used for our main analyses and interpretations. Finally, we compared the parasitism TPC to the host and parasite trait TPCs measured in isolation.

We used R version 4.2.1 for all statistical analyses and for figure generation (R Core Team, 2022). See Appendix S1 for additional details and R packages used.

Results

Does infection occurrence vary with temperature across the species range?

Infection occurrence followed a hump-shaped pattern along the surveyed temperature gradient, peaking at 9.4ºC mean rainy season temperature (Figure 2). Mean temperature^2 and year were significant predictors of *L. clarki* infection presence (Table 1). Quadratic models fit individually for infection occurrence in each year peaked at 10.0ºC in 2022 and 9.2ºC in 2023, but the interactions between year and both temperature variables were not statistically significant, indicating that the temperature – infection relationship did not vary between years (Table 1). Geographically, infections were common in northern California and southern Oregon and rarer at the warm and cold ends of the surveyed temperature gradient in southern California and northern Washington, respectively (Figure 1).

Of the two sampling years, 2023 was cooler and wetter and had a higher percentage of infected tree holes (29.7%, N = 431) compared to 2022 (12.5%, N = 320) (Figure 2) (NOAA National Centers for Environmental Information, 2022; 2023). Mean tree hole habitat temperatures logged by iButtons (N = 32 successfully retrieved) were strongly correlated with and were not systematically warmer or colder than mean PRISM air temperature estimates (linear regression intercept = -0.41, t- SE = 1.76, t-value = -0.24, p-value = 0.82; slope = 0.95, SE = 0.1, t-value = 9.11, p-value = 3.86×10^{-10}) (mean temperature difference = 1.3ºC, SD = 2.6ºC) (Appendix S2: Figure S1). Additional details are provided in Appendix S2.

Does the thermal response of the host – parasite interaction depend on the host population?

We found similar thermal optima, minima and maxima across the six host populations in the infection experiment within each of the three measured interaction outcomes of infection,

294 melanization of parasites, and mortality (Figure 3; Appendix S2: Figures S2-S11; Tables S3-S7).
295 Although the mean estimated T_{opt}, T_{min}, and T_{max} varied slightly among populations for each
296 trait, all 95% credible intervals across populations for each outcome x parameter combination
297 overlapped. Therefore, we combined the data for all host populations to estimate broadly
298 representative TPCs for the host – parasite interaction, with reduced uncertainty compared to the
299 population-specific TPCs (Figure 4; Appendix S2: Figure S12; Table S9). The only trait in which
300 we observed clear intraspecific variation was in mortality around 10ºC, which was higher in one
301 intermediate climate population (Big Sur (BIG)) compared to the other (Woodside (JR)) and to
302 one cold climate population (Eugene (EUG)) (Figure S13).
303
304 *How do different components of the host – parasite interaction relate to the overall thermal*
305 *sensitivity of parasitism?*
306 Although free-living parasite population growth was maximized at warm temperatures, infection
307 and parasite-induced mortality peaked at significantly colder temperatures, corresponding to
308 conditions that suppressed host defense mechanisms, namely the melanization immune response
309 and larval development speed (Figure 4). Specifically, the experimentally measured initial
310 infection rate peaked at 10ºC (95% CI: 8.7 ºC, 11.3 ºC), and the total infection rate peaked at
311 8.4ºC (95% CI: 6.8 ºC, 9.4 ºC), much lower temperatures than the 19.5ºC (95% CI: 18.9 ºC, 20.2
312 ºC) optimum for free-living parasite population growth, but near the field-estimated 10.0ºC and
313 9.2ºC peaks in 2022 and 2023, respectively (Figure 4A; Appendix S2: Figure S12; Tables S8-9).
314 The mechanically assayed host melanization immune response increased with temperature up to
315 20ºC, where it plateaued (Figure 4A; Appendix S2: Table S10). At warmer temperatures,
316 attacking parasites faced not only a stronger host immune response, but also shorter time

317 windows in which to infect hosts without being shed with the cuticle during larval molting and
318 pupation or eaten by later larval instars. The time to the first observed pupation shortened as the
319 temperature increased, occurring after 9 days at 28ºC compared to 57 days at 7ºC (Figure 4B),
320 consistent with previously measured *Ae. sierrensis* larval development rate TPCs that peaked at
321 27.7ºC (Couper et al., 2024). Consequently, rapid pupation interrupted upward trajectories of
322 infection and mortality at intermediate temperatures, contributing to the decline in parasitism
323 above 11ºC, and to the lower T_{opt} of total compared to initial infection. At colder temperatures,
324 additional opportunities for parasitism were also generated as infected host deaths beginning in
325 the third week of the experiment maintained higher *L. clarki* densities throughout extended host
326 developmental periods (Figure S14). In comparison, at the warmest temperature with infections
327 (18ºC), the contributions of infected host deaths to subsequent transmission were limited by their
328 rarity and proximity to the onset of pupation.

329 **Discussion**

330 In this study, we used complementary field observations and lab experiments to understand
331 how temperature affects a host-parasite interaction across a large, climatically variable species
332 range. We found that infection peaked at sites with intermediate temperatures (9.4ºC) in the field
333 across two sampling years and was higher in a colder, wetter year, aligning with the unimodal
334 temperature-dependence of infection measured in the lab, which peaked at 10ºC. This reflects the
335 interacting thermal biology of multiple mosquito and ciliate traits, which together led to an
336 optimal temperature for parasitism (8-10ºC for total versus initial infection) that was colder than
337 the optimal temperature for free-living parasite performance (19.5ºC). Infection rates of
338 mosquito populations from different climates had similar thermal responses in the lab, and a
339 single TPC described the infection process across the entire surveyed area. These findings

340 suggest that for systems with strong temperature dependence, TPCs measured under simplified
341 lab conditions can capture patterns of parasitism across large geographic temperature gradients
342 in complex natural settings, by quantifying the underlying thermal biology mechanisms.
343
344 *Lab experiments capture nonlinear parasitism thermal responses in the field*
345 The results add to evidence that temperature nonlinearly affects parasitism not only in the
346 lab, but also in nature, making laboratory and field studies that are designed to capture nonlinear
347 temperature effects valuable tools for understanding disease risk (Dudney et al., 2021; Kirk et al.,
348 2024; Shocket, Ryan et al., 2018; Shocket, Strauss et al., 2018). However, despite the similarities
349 between the field observations and the lab-measured parasitism TPC, we cannot rule out the
350 influence of other factors. For example, while the role of precipitation in this system has not been
351 assessed, the colder survey year with higher infection prevalence was also wetter, suggesting that
352 precipitation patterns that determined when and for how long tree holes were water-filled may
353 have also affected the potential for parasitism to occur. Beyond mean temperature differences,
354 heatwaves or cold snaps occurring during key points in the host – parasite interaction may have
355 also contributed to interannual variation in infection presence (Claar & Wood, 2020; Altman et
356 al., 2016). These limitations should be addressed with field experiments that manipulate
357 temperatures in natural tree holes at different latitudes or elevations; lab experiments that
358 incorporate additional environmental complexity; and long term repeated yearly sampling of the
359 same tree holes.
360
361 *Intraspecific variation*

362 Very few studies investigate the impact of local thermal adaptation on species distributions
363 and host – parasite interactions, a gap often noted in the literature (Sternberg & Thomas, 2014;
364 Urban et al., 2016; Couper et al., 2021; Aleuy et al., 2023). In addressing this gap, we did not
365 find evidence of local temperature adaptation affecting infection patterns across temperatures in
366 the lab or the field. While our laboratory experiment specifically assessed host local adaptation,
367 the invariant temperature dependence of infection we observed is consistent with the similar
368 temperature-infection relationship in the field, and with our previous work comparing sympatric
369 and allopatric host – parasite interactions. Specifically, for nine *Ae. sierrensis* and *L. clarki*
370 populations with free-living parasite T_{opt} ranging from 16.5ºC to 23.5ºC, infection rates measured
371 at three temperatures peaked at the intermediate temperature of 12.5ºC, substantially cooler than
372 the free-living growth optima (Lyberger et al., 2024). Cumulatively, these findings suggest that
373 although both *Ae. sierrensis* pupal development and *L. clarki* free-living population growth rates
374 are locally adapted to temperature, this intraspecific variation is unlikely to directly affect host –
375 parasite interactions. (Lyberger et al., 2024; Couper et al., 2024; Ismail et al., 2023). Variability
376 in the infection T_{opt} should be further tested through TPC experiments with additional host –
377 parasite population pairs, but differences in factors such as host fitness and adaptation to
378 parasites may be more important sources of intraspecific variation in parasite impacts. For
379 example, in this experiment, the mosquito population with the lowest egg hatching rate, BIG, had
380 a higher mortality rate near the infection T_{opt} compared to two other populations; and in previous
381 experiments, individual host populations varied in their susceptibility to different parasite strains
382 (Ismail et al., 2023; Lyberger et al., 2024)
383 Importantly, this is one of the only ectothermic host – parasite systems for which interaction
384 thermal sensitivity has been assessed for populations from different climates, along with a

stickleback – tapeworm system in which effects of temperature on parasitism were similar among four study populations collected from across a similar geographic temperature gradient (Franke et al., 2019). Notably, intraspecific variation in parasitism temperature sensitivity has been shown for levels of biological organization both above and below the population level that we assessed, for *Batrachochytrium dendrobatitis* infection both among different frog host species, and among salamander host color morphs within a single population (Cohen et al., 2017; Venesky et al., 2022). However, if population thermal sensitivities of parasitism are commonly consistent across species ranges, broadly applicable TPCs should be easily attainable for the many host – parasite systems that are amenable to laboratory studies, and field studies may also be able to capture nonlinear responses of parasitism to temperature.

Mechanisms of parasitism temperature dependence

Our finding that parasitism peaked at temperatures that constrained host development and defense—rather than at the thermal optimum for parasite growth and attack—aligns with theory on the thermal biology of biotic interactions. Thermal asymmetry theory posits that parasitism peaks at temperatures where parasites outperform hosts, which may differ from optimal temperatures for the parasites themselves (Dell et al., 2014; Cohen et al., 2017). Our study supports the value of approaching this problem as the outcome of multiple interacting host and parasite traits with varying thermal responses (Paull et al., 2012; Shocket et al., 2018; Sun et al., 2023).

Conclusions

Overall, our characterization of the temperature – infection relationship of the *Ae. sierrensis* host – *L. clarki* parasite interaction across settings demonstrates how controlled lab experiments can be paired with large-scale field observations to understand the complex thermal biology of parasitism. Climate warming is expected to cause geographic contractions, expansions, and shifts in host thermal refuges from disease (Altizer et al., 2013; Gsell et al., 2023). Our results suggest that parasite burdens on *Ae. sierrensis* may decline at southern latitudes and low elevations as thermally suitable conditions for parasitism shift northwards and upwards into areas where cold conditions currently limit *L. clarki* infections. Whether the distribution of parasitism ultimately tracks climate warming will depend on multiple factors, including parasite dispersal, the pace of thermal adaptation in host and parasite traits that allow local populations of each species to persist individually, and the effects of other environmental changes in conjunction with increasing mean temperatures, such as increasingly extreme precipitation patterns (Swain et al., 2018). Understanding how temperature affects parasitism in inherently complex and variable natural systems remains a pressing problem with broad implications for current and future disease risk management. Simple pairings of field surveys and lab experiments can offer straightforward means for approaching this challenge.

Acknowledgments

Otto Seppälä, Jan Washburn, Nona Chiariello, and Angie Nakano played critical roles in establishing the study system. Our field sampling and mosquito rearing efforts were made possible by assistance from staff at vector control agencies for the California counties of San Mateo, Santa Clara, Marin-Sonoma, Solano, Alameda, Shasta, Placer, Santa Barbara, and Riverside; Jasper Ridge Biological Preserve ‘Ootchamin ‘Ooyakma; the UC Reserves at

Emerson Oaks, Dawson Los Monos Canyon, and Hopland; and Andrew Rivera of Clarke Pest Control. Mordecai lab members helped with setting up the infection experiment. JEF was funded by the Bing-Mooney Fellowship and the ARCS Foundation. EAM and MCL were supported by the National Institutes of Health (R35GM133439 and R01AI168097). EAM was supported by the National Science Foundation (DEB-2011147 with Fogarty International Center), the National (R01AI102918), the Stanford Woods Institute for the Environment, the Stanford Center for Innovation in Global Health, and the Stanford Doerr School of Sustainability. KL was funded by the NSF Postdoctoral Research Fellowships in Biology Program under Grant No. 2208947. LIC was funded by the NSF Postdoctoral Research Fellowship in Biology. MCL was supported by a Stanford PRISM Baker Fellowship.

Conflict of Interest Statement

The authors declare no conflict of interest.

References

Ahrens, Collin W., Richard A. Mazanec, Trudy Paap, Katinka X. Ruthrof, Anthea Challis, Giles Hardy, Margaret Byrne, David T. Tissue, and Paul D. Rymer. 2019. "Adaptive Variation for Growth and Resistance to a Novel Pathogen along Climatic Gradients in a Foundation Tree." *Evolutionary Applications* 12 (6): 1178–90. https://doi.org/10.1111/eva.12796.

Aleuy, O. Alejandro, Stephanie J. Peacock, Péter K. Molnár, Kathreen E. Ruckstuhl, and Susan J. Kutz. 2023. "Local Thermal Adaptation and Local Temperature Regimes Drive the Performance of a Parasitic Helminth under Climate Change: The Case of *Marshallagia marshalli* from Wild Ungulates." *Global Change Biology* 29 (22): 6217–33. https://doi.org/10.1111/gcb.16918.

Altman, Karie A., Sara H. Paull, Pieter T. J. Johnson, et al. 2016. "Host and Parasite Thermal

Acclimation Responses Depend on the Stage of Infection." *Journal of Animal Ecology* 85 (4): 1014–24. https://doi.org/10.1111/1365-2656.12510.

Altizer, Sonia, Richard S. Ostfeld, Pieter T. J. Johnson, Susan Kutz, and C. Drew Harvell. 2013. "Climate Change and Infectious Diseases: From Evidence to a Predictive Framework." *Science* 341 (6145): 514–19. https://doi.org/10.1126/science.1239401.

Angilletta, Michael J. 2009. *Thermal Adaptation: A Theoretical and Empirical Synthesis*. Oxford, UK: Oxford Univ. Press

Bates, Douglas, Martin Maechler, Ben Bolker, and Steven Walker. 2003. "Lme4: Linear Mixed-Effects Models Using 'Eigen' and S4." https://doi.org/10.32614/CRAN.package.lme4.

Boots, M. 2000. "Density-Independent Resource Limitation and the Transmission of an Insect Pathogen." *Oecologia* 124 (2): 172–75. https://doi.org/10.1007/s004420050004.

Broberg, Leonard E., and William E. Bradshaw. 1997. "*Lambornella clarki* (Ciliophora: Tetrahymenidae) Resistance in *Aedes sierrensis* (Diptera: Culicidae): Population Differentiation in a Quantitative Trait and Allozyme Loci." *Journal of Medical Entomology* 34 (1): 38–45. https://doi.org/10.1093/jmedent/34.1.38.

Brown, Joel J., Mercedes Pascual, Michael C. Wimberly, Leah R. Johnson, and Courtney C. Murdock. 2023. "Humidity – The Overlooked Variable in the Thermal Biology of Mosquito-Borne Disease." *Ecology Letters* 26 (7): 1029–49. https://doi.org/10.1111/ele.14228.

Christensen, Bruce M., Jianyong Li, Cheng-Chen Chen, and Anthony J. Nappi. 2005. "Melanization Immune Responses in Mosquito Vectors." *Trends in Parasitology* 21 (4): 192–99. https://doi.org/10.1016/j.pt.2005.02.007.

Claar, Danielle C., and Chelsea L. Wood. 2020. "Pulse Heat Stress and Parasitism in a Warming World." *Trends in Ecology & Evolution* 35 (8): 704–15. https://doi.org/10.1016/j.tree.2020.04.002.

Clark, T.B., and D.G. Brandl. 1976. "Observations on the Infection of *Aedes sierrensis* by a Tetrahymenine Ciliate." *Journal of Invertebrate Pathology* 28 (3): 341–49. https://doi.org/10.1016/0022-2011(76)90009-4.

Cohen, Jeremy M., Matthew D. Venesky, Erin L. Sauer, David J. Civitello, Taegan A. McMahon, Elizabeth A. Roznik, and Jason R. Rohr. 2017. "The Thermal Mismatch Hypothesis Explains Host Susceptibility to an Emerging Infectious Disease." *Ecology Letters* 20 (2): 184–93. https://doi.org/10.1111/ele.12720.

Couper, Lisa I., Johannah E. Farner, Jamie M. Caldwell, Marissa L. Childs, Mallory J. Harris, Devin G. Kirk, Nicole Nova, et al. 2021. "How Will Mosquitoes Adapt to Climate Warming?" *eLife* 10 (August):e69630. https://doi.org/10.7554/eLife.69630.

Couper, Lisa I., Johannah E. Farner, Kelsey P. Lyberger, Alexandra S. Lee, and Erin A. Mordecai. 2024. "Mosquito Thermal Tolerance Is Remarkably Constrained across a Large Climatic Range." *Proceedings of the Royal Society B: Biological Sciences* 291 (2015): 20232457. https://doi.org/10.1098/rspb.2023.2457.

Cruz-Loya, Mauricio, Erin A. Mordecai, and Van M. Savage. 2024. "A Flexible Model for Thermal Performance Curves." *bioRxiv*, January, 2024.08.01.605695. https://doi.org/10.1101/2024.08.01.605695.

Darsie, Richard F., and Ronald A. Ward. 2005. *Identification and Geographical Distribution of the Mosquitoes of North America, North of Mexico*. University Press of Florida.

Dell, Anthony I., Samraat Pawar, and Van M. Savage. 2014. "Temperature Dependence of Trophic Interactions Are Driven by Asymmetry of Species Responses and Foraging Strategy." *Journal of Animal Ecology* 83 (1): 70–84. https://doi.org/10.1111/1365-2656.12081.

Dudney, Joan, Claire E. Willing, Adrian J. Das, Andrew M. Latimer, Jonathan C. B. Nesmith, and John J. Battles. 2021. "Nonlinear Shifts in Infectious Rust Disease Due to Climate Change." *Nature Communications* 12 (1): 5102. https://doi.org/10.1038/s41467-021-25182-6.

Franke, Frederik, Nadja Raifarth, Joachim Kurtz, and Jörn P. Scharsack. 2019. "Consequences of Divergent Temperature Optima in a Host–Parasite System." *Oikos* 128 (6): 869–80. https://doi.org/10.1111/oik.05864.

Gaitán-Espitia, Juan Diego, Leonardo D. Bacigalupe, Tania Opitz, Nelson A. Lagos, Tania Timmermann, and Marco A. Lardies. 2014. "Geographic Variation in Thermal Physiological Performance of the Intertidal Crab *Petrolisthes violaceus* along a Latitudinal Gradient." *Journal of Experimental Biology* 217 (24): 4379–86. https://doi.org/10.1242/jeb.108217.

Gehman, Alyssa-Lois M., Richard J. Hall, and James E. Byers. 2018. "Host and Parasite Thermal Ecology Jointly Determine the Effect of Climate Warming on Epidemic Dynamics." *Proceedings of the National Academy of Sciences* 115 (4): 744–49. https://doi.org/10.1073/pnas.1705067115.

Gsell, Alena S., Arjen Biere, Wietse de Boer, Irene de Bruijn, Götz Eichhorn, Thijs Frenken, Stefan Geisen, et al. 2023. "Environmental Refuges from Disease in Host–Parasite

Interactions under Global Change." *Ecology* 104 (4): e4001. https://doi.org/10.1002/ecy.4001.

Hall, Spencer R., Joseph L. Simonis, Roger M. Nisbet, Alan J. Tessier, and Carla E. Cáceres. 2009. "Resource Ecology of Virulence in a Planktonic Host-Parasite System: An Explanation Using Dynamic Energy Budgets." *The American Naturalist* 174 (2): 149–62. https://doi.org/10.1086/600086.

Hartig, Florian. 2017. "Package 'Dharma.'" *R Package*.

Ismail, Sherine, Johannah Farner, Lisa Couper, Erin Mordecai, and Kelsey Lyberger. 2023. "Temperature and Intraspecific Variation Affect Host–Parasite Interactions." *Oecologia*, November. https://doi.org/10.1007/s00442-023-05481-z.

Jordan, R. G., and W. E. Bradshaw. 1978. "Geographic Variation in the Photoperiodic Response of the Western Tree-Hole Mosquito, *Aedes sierrensis*." *Annals of the Entomological Society of America* 71 (4): 487–90. https://doi.org/10.1093/aesa/71.4.487.

Jordan, Robert G. 1980a. "Embryonic Diapause in Three Populations of the Western Tree Hole Mosquito, *Aedes sierrensis*." *Annals of the Entomological Society of America* 73 (4): 357–59. https://doi.org/10.1093/aesa/73.4.357.

———. 1980b. "Geographic Differentiation in the Development *of Aedes sierrensis* (Diptera: Culicidae) in Nature." *The Canadian Entomologist* 112 (2): 205–10. https://doi.org/10.4039/Ent112205-2.

Jurriaans, S., and M. O. Hoogenboom. 2019. "Thermal Performance of Scleractinian Corals along a Latitudinal Gradient on the Great Barrier Reef." *Philosophical Transactions of the Royal Society B: Biological Sciences* 374 (1778): 20180546. https://doi.org/10.1098/rstb.2018.0546.

Kirk, Devin, Natalie Jones, Stephanie Peacock, Jessica Phillips, Péter K. Molnár, Martin Krkošek, and Pepijn Luijckx. 2018. “Empirical Evidence That Metabolic Theory Describes the Temperature Dependency of Within-Host Parasite Dynamics.” *PLOS Biology* 16 (2): e2004608. https://doi.org/10.1371/journal.pbio.2004608.

Kirk, Devin, Samantha Straus, Marissa L. Childs, Mallory Harris, Lisa Couper, T. Jonathan Davies, Coreen Forbes, et al. 2024. “Temperature Impacts on Dengue Incidence Are Nonlinear and Mediated by Climatic and Socioeconomic Factors: A Meta-Analysis.” *PLOS Climate* 3 (3): e0000152. https://doi.org/10.1371/journal.pclm.0000152.

Kutz, S. J., E. P. Hoberg, L. Polley, and E. J. Jenkins. 2005. “Global Warming Is Changing the Dynamics of Arctic Host-Parasite Systems.” *Proceedings: Biological Sciences* 272 (1581): 2571–76.

Labaude, Sophie, Yannick Moret, Frank Cézilly, Charel Reuland, and Thierry Rigaud. 2017. “Variation in the Immune State of *Gammarus pulex* (Crustacea, Amphipoda) According to Temperature: Are Extreme Temperatures a Stress?” *Developmental & Comparative Immunology* 76 (November):25–33. https://doi.org/10.1016/j.dci.2017.05.013.

Laughton, Alice M., Cian O. O’Connor, and Robert J. Knell. 2017. “Responses to a Warming World: Integrating Life History, Immune Investment, and Pathogen Resistance in a Model Insect Species.” *Ecology and Evolution* 7 (22): 9699–9710. https://doi.org/10.1002/ece3.3506.

Luković, Jelena, John C. H. Chiang, Dragan Blagojević, and Aleksandar Sekulić. 2021. “A Later Onset of the Rainy Season in California.” *Geophysical Research Letters* 48 (4): e2020GL090350. https://doi.org/10.1029/2020GL090350.

Lyberger, Kelsey, Johannah Farner, Lisa Couper, and Erin A. Mordecai. 2024. "A Mosquito Parasite Is Locally Adapted to Its Host but Not Temperature." *The American Naturalist* 204 (2): 121–32. https://doi.org/10.1086/730522.

Martin, Lindsay E., and Julián F. Hillyer. 2024. "Higher Temperature Accelerates the Aging-Dependent Weakening of the Melanization Immune Response in Mosquitoes." *PLOS Pathogens* 20 (1): e1011935. https://doi.org/10.1371/journal.ppat.1011935.

Mazé-Guilmo, Elise, Simon Blanchet, Olivier Rey, Nicolas Canto, and Géraldine Loot. 2016. "Local Adaptation Drives Thermal Tolerance among Parasite Populations: A Common Garden Experiment." *Proceedings of the Royal Society B: Biological Sciences* 283 (1830): 20160587. https://doi.org/10.1098/rspb.2016.0587.

Mordecai, Erin A., Jamie M. Caldwell, Marissa K. Grossman, Catherine A. Lippi, Leah R. Johnson, Marco Neira, Jason R. Rohr, et al. 2019. "Thermal Biology of Mosquito-borne Disease." *Ecology Letters*, July, ele.13335. https://doi.org/10.1111/ele.13335.

Mordecai, Erin A., Jeremy M. Cohen, Michelle V. Evans, Prithvi Gudapati, Leah R. Johnson, Catherine A. Lippi, Kerri Miazgowicz, et al. 2017. "Detecting the Impact of Temperature on Transmission of Zika, Dengue, and Chikungunya Using Mechanistic Models." *PLOS Neglected Tropical Diseases* 11 (4): e0005568. https://doi.org/10.1371/journal.pntd.0005568.

Mordecai, Erin A., Krijn P. Paaijmans, Leah R. Johnson, Christian Balzer, Tal Ben-Horin, Emily de Moor, Amy McNally, et al. 2013. "Optimal Temperature for Malaria Transmission Is Dramatically Lower than Previously Predicted." *Ecology Letters* 16 (1): 22–30. https://doi.org/10.1111/ele.12015.

Murdock, C. C., Krijn P. Paaijmans, Andrew S. Bell, Jonas G. King, Julián F. Hillyer, Andrew F. Read, and Matthew B. Thomas. 2012. "Complex Effects of Temperature on Mosquito Immune Function." *Proceedings of the Royal Society B: Biological Sciences* 279 (1741): 3357–66. https://doi.org/10.1098/rspb.2012.0638.

NOAA National Centers for Environmental Information. 2022. "Monthly National Climate Report for 2022." https://www.ncei.noaa.gov/access/monitoring/monthly-report/national/202408.

———. 2023. "Monthly National Climate Report for 2023." https://www.ncei.noaa.gov/access/monitoring/monthly-report/national/202408.

Padfield, Daniel, Meaghan Castledine, and Angus Buckling. 2020. "Temperature-Dependent Changes to Host–Parasite Interactions Alter the Thermal Performance of a Bacterial Host." *The ISME Journal* 14 (2): 389–98. https://doi.org/10.1038/s41396-019-0526-5.

Palmer-Young, Evan C., Lyna Ngor, Rodrigo Burciaga Nevarez, Jason A. Rothman, Thomas R. Raffel, and Quinn S. McFrederick. 2019. "Temperature Dependence of Parasitic Infection and Gut Bacterial Communities in Bumble Bees." *Environmental Microbiology* 21 (12): 4706–23. https://doi.org/10.1111/1462-2920.14805.

Paull, Sara H., Bryan E. LaFonte, and Pieter T. J. Johnson. 2012. "Temperature-Driven Shifts in a Host-Parasite Interaction Drive Nonlinear Changes in Disease Risk." *Global Change Biology* 18 (12): 3558–67. https://doi.org/10.1111/gcb.12018.

Penczykowski, Rachel M., Spencer R. Hall, David J. Civitello, and Meghan A. Duffy. 2014. "Habitat Structure and Ecological Drivers of Disease." *Limnology and Oceanography* 59 (2): 340–48. https://doi.org/10.4319/lo.2014.59.2.0340.

Petzoldt, Thomas. 2022. "R Package Growthrates."

Praskievicz, Sarah, and Heejun Chang. 2009. “Winter Precipitation Intensity and ENSO/PDO Variability in the Willamette Valley of Oregon.” *International Journal of Climatology* 29 (13): 2033–39. https://doi.org/10.1002/joc.1838.

PRISM Climate Group, and Oregon State University. 2021. “PRISM Gridded Climate Data.” https://prism.oregonstate.edu.

Ragonese, Isabella G., Maya R. Sarkar, Richard J. Hall, and Sonia Altizer. 2024. “Extreme Heat Reduces Host and Parasite Performance in a Butterfly–Parasite Interaction.” *Proceedings of the Royal Society B: Biological Sciences* 291 (2015): 20232305. https://doi.org/10.1098/rspb.2023.2305.

R Core Team. 2022. R: A language and environment for statistical computing. R Foundation for Statistical Computing, Vienna, Austria. https://www.R-project.org/.

Ryan, Sadie J., Colin J. Carlson, Erin A. Mordecai, and Leah R. Johnson. 2019. “Global Expansion and Redistribution of *Aedes*-Borne Virus Transmission Risk with Climate Change.” *PLOS Neglected Tropical Diseases* 13 (3): e0007213. https://doi.org/10.1371/journal.pntd.0007213.

Seppälä, Otto, Katri Liljeroos, Anssi Karvonen, and Jukka Jokela. 2008. “Host Condition as a Constraint for Parasite Reproduction.” *Oikos* 117 (5): 749–53. https://doi.org/10.1111/j.0030-1299.2008.16396.x.

Shah, Melisa M., Amy R. Krystosik, Bryson A. Ndenga, Francis M. Mutuku, Jamie M. Caldwell, Victoria Otuka, Philip K. Chebii, et al. 2019. “Malaria Smear Positivity among Kenyan Children Peaks at Intermediate Temperatures as Predicted by Ecological Models.” *Parasites & Vectors* 12 (1): 288. https://doi.org/10.1186/s13071-019-3547-z.

632 Shocket, Marta S., Alexander T. Strauss, Jessica L. Hite, Maja Šljivar, David J. Civitello,
633 Meghan A. Duffy, Carla E. Cáceres, and Spencer R. Hall. 2018. "Temperature Drives
634 Epidemics in a Zooplankton-Fungus Disease System: A Trait-Driven Approach Points to
635 Transmission via Host Foraging." *The American Naturalist* 191 (4): 435–51.
636 https://doi.org/10.1086/696096.
637 Shocket, Marta S., Anna B. Verwillow, Mailo G. Numazu, Hani Slamani, Jeremy M. Cohen,
638 Fadoua El Moustaid, Jason Rohr, Leah R. Johnson, and Erin A. Mordecai. 2020.
639 "Transmission of West Nile and Five Other Temperate Mosquito-Borne Viruses Peaks at
640 Temperatures between 23°C and 26°C." *eLife* 9 (September):e58511.
641 https://doi.org/10.7554/eLife.58511.
642 Shocket, Marta S., Sadie J. Ryan, and Erin A. Mordecai. 2018. "Temperature Explains Broad
643 Patterns of Ross River Virus Transmission." *eLife* 7 (August):e37762.
644 https://doi.org/10.7554/eLife.37762.
645 Sinclair, Brent J., Caroline M. Williams, and John S. Terblanche. 2012. "Variation in Thermal
646 Performance among Insect Populations." *Physiological and Biochemical Zoology* 85 (6):
647 594–606. https://doi.org/10.1086/665388.
648 Sternberg, Eleanore D., and Matthew B. Thomas. 2014. "Local Adaptation to Temperature and
649 the Implications for Vector-Borne Diseases." *Trends in Parasitology* 30 (3): 115–22.
650 https://doi.org/10.1016/j.pt.2013.12.010.
651 Sun, Syuan-Jyun, Marcin K. Dziuba, Riley N. Jaye, and Meghan A. Duffy. 2023. "Temperature
652 Modifies Trait-Mediated Infection Outcomes in a *Daphnia*–Fungal Parasite System."
653 *Philosophical Transactions of the Royal Society B: Biological Sciences* 378 (1873):
654 20220009. https://doi.org/10.1098/rstb.2022.0009.

Suwanchaichinda, Chansak, and Susan M. Paskewitz. 1998. "Effects of Larval Nutrition, Adult Body Size, and Adult Temperature on the Ability of *Anopheles gambiae* (Diptera: Culicidae) to Melanize Sephadex Beads." *Journal of Medical Entomology* 35 (2): 157–61. https://doi.org/10.1093/jmedent/35.2.157.

Swain, Daniel L., Baird Langenbrunner, J. David Neelin, and Alex Hall. 2018. "Increasing Precipitation Volatility in Twenty-First-Century California." *Nature Climate Change* 8 (5): 427–33. https://doi.org/10.1038/s41558-018-0140-y.

Taylor, Rachel A., Sadie J. Ryan, Catherine A. Lippi, David G. Hall, Hossein A. Narouei-Khandan, Jason R. Rohr, and Leah R. Johnson. 2019. "Predicting the Fundamental Thermal Niche of Crop Pests and Diseases in a Changing World: A Case Study on Citrus Greening." *Journal of Applied Ecology*, July, 1365-2664.13455. https://doi.org/10.1111/1365-2664.13455.

Tesla, Blanka, Leah R. Demakovsky, Erin A. Mordecai, Sadie J. Ryan, Matthew H. Bonds, Calistus N. Ngonghala, Melinda A. Brindley, and Courtney C. Murdock. 2018. "Temperature Drives Zika Virus Transmission: Evidence from Empirical and Mathematical Models." *Proceedings of the Royal Society B: Biological Sciences* 285 (1884): 20180795. https://doi.org/10.1098/rspb.2018.0795.

Thomas, Matthew B., and Simon Blanford. 2003. "Thermal Biology in Insect-Parasite Interactions." *Trends in Ecology & Evolution* 18 (7): 344–50. https://doi.org/10.1016/S0169-5347(03)00069-7.

Urban, M. C., G. Bocedi, A. P. Hendry, J.-B. Mihoub, G. Pe'er, A. Singer, J. R. Bridle, et al. 2016. "Improving the Forecast for Biodiversity under Climate Change." *Science* 353 (6304): aad8466. https://doi.org/10.1126/science.aad8466.

Venesky, Matthew D., Joseph DeMarchi, Cari Hickerson, and Carl D. Anthony. 2022. "Does the Thermal Mismatch Hypothesis Predict Disease Outcomes in Different Morphs of a Terrestrial Salamander?" *Journal of Experimental Zoology Part A: Ecological and Integrative Physiology*, 1–10. https://doi.org/10.1002/jez.2581.

Washburn, J., M. Gross, D. Mercer, and Anderson. 1988. "Predator-Induced Trophic Shift of a Free-Living Ciliate: Parasitism of Mosquito Larvae by Their Prey." *Science* 240 (4856): 1193–95. https://doi.org/10.1126/science.3131877.

Washburn, Jan O., and John R. Anderson. 1986. "Distribution of *Lambornella clarki* (Ciliophora: Tetrahymenidae) and Other Mosquito Parasites in California Treeholes." *Journal of Invertebrate Pathology* 48 (3): 296–309. https://doi.org/10.1016/0022-2011(86)90058-3.

Washburn, Jan O., John R. Anderson, and David R. Mercer. 1991. "Parasitism of Newly-Hatched *Aedes sierrensis* (Diptera: Culicidae) Larvae by *Lambornella clarki* (Ciliophora: Tetrahymenidae) Following Habitat Flooding." *Journal of Invertebrate Pathology* 58 (1): 67–74. https://doi.org/10.1016/0022-2011(91)90163-K.

693 **Tables**

694 **Table 1. Results of a generalized linear mixed-effects model with tree hole infection status**

695 **as the dependent variable and mean annual temperature, mean annual temperature^2, and**

696 **survey year as fixed effects, and tree hole ID as a random effect.**

697

Predictor	Estimate	Standard error	Z-value	p-value
Mean annual temperature	-0.22	0.22	-1.01	3.13×10^{-1}
Mean annual temperature^2	-0.43	0.21	-2.01	**4.45×10^{-2}**
Survey year	1.31	0.34	3.90	**9.5×10^{-5}**
*Mean annual temperature * survey year*	-0.45	0.26	-1.72	8.5×10^{-2}
*Mean annual temperature^2 * survey year*	-0.127	0.247	-0.52	6.34×10^{-1}

698

699 P-values < 0.05 are displayed in bold to highlight statistical significance.

700

701 **Figure captions**

702 **Figure 1. Tree holes were surveyed, and experimental host and parasite populations reared,**
703 **from across a large geographic temperature gradient on the western coast of the United**
704 **States during the (A) 2022 and (B) 2023 rainy seasons.** The mapped color gradient shows
705 mean temperature during the rainy season in Washington, Oregon, and California, USA, from the
706 4 km PRISM climate dataset. Points show the locations of 507 total surveyed tree holes. *L. clarki*
707 infection presence is indicated by black points, and absence by white points. In (A), colored
708 ovals indicate the source locations of the six host populations used in the infection experiment
709 (from north to south: EUG = Eugene, OR; JR = Woodside, CA; FRS = Shaver Lake, CA; BIG =
710 Big Sur, CA; WHIT = Trabuco Canyon, CA; CAS = San Juan Capistrano, CA); the gray oval
711 shows the host population used in the melanization response experiment (PAR = Paso Robles,
712 CA); and the gray rectangle shows the source location of the ciliate parasite culture used in the
713 infection experiment (Marin = Novato, CA). In (B), green outlines indicate tree holes in which
714 iButtons logged temperature data during the year between the two sampling visits.

715 **Figure 2. Infection probability followed a consistent hump-shaped relationship with mean**
716 **temperature during the rainy season, and was higher overall in 2023 compared to 2022. (A)**
717 Counts of infected (black) and uninfected (gray) tree holes across the climate gradient in each
718 survey year. **(B)** Generalized linear mixed-effects model predictions of infection probability by
719 temperature and year are plotted across the surveyed climate gradient for each year of the field
720 survey. The solid and dashed lines show the mean model predictions for 2022 and 2023,
721 respectively, and the shading shows the 95% confidence intervals.

722 **Figure 3. Thermal responses of host – parasite interaction outcomes were similar among**
723 **host populations from warm, intermediate, and cold source climates.** For each outcome

724 measured in the infection experiment, mean estimated TPCs for each of six host populations are
725 shown (lines) with 95% credible intervals (shading). The left column shows **(A)** initial infection
726 and **(B)** parasite melanization responses up to the third experiment checkpoint, when the first
727 deaths of infected larvae released additional parasites into the environment. The right column
728 shows the **(C)** total infection, **(D)** parasite melanization, and **(E)** parasite-induced mortality rates
729 across temperatures at the end of the experiment. Mortality rates were significantly higher near
730 10 ºC for population BIG compared to populations JR and EUG. The TPCs shown here are
731 presented individually, with the experiment data, in Appendix S2 (Figures S2, S4, S6, S8, S10).
732 **Figure 4. Experimental infections were most likely to occur at cold incubation**
733 **temperatures where the host melanization response and development were suppressed. (A)**
734 Points show mean values, error bars show +/- 1 SE, lines show mean estimated TPCs, and
735 shading shows 95% credible intervals for key host – parasitism interaction outcomes and
736 processes: free-living parasite population growth (green); the host mechanically stimulated
737 melanization immune response (black); the initial infection rate (light pink), calculated up to the
738 first fatality at each temperature; the total infection rate (dark pink); and total mortality (gray)
739 calculated up to the first pupation at each temperature. The infection data shown include all host
740 populations in the infection experiment. **(B)** Infection (top; dark pink), parasite-induced mortality
741 (middle; light gray), and parasite melanization (bottom; dark gray) counts are plotted over time
742 for each temperature used in the infection experiment. Colored points show data from individual
743 microcosms, and black points and lines show mean trajectories +/- 1 SE. For each temperature,
744 the final experiment checkpoint was at the time of the first observed pupation.
745

Figure 1

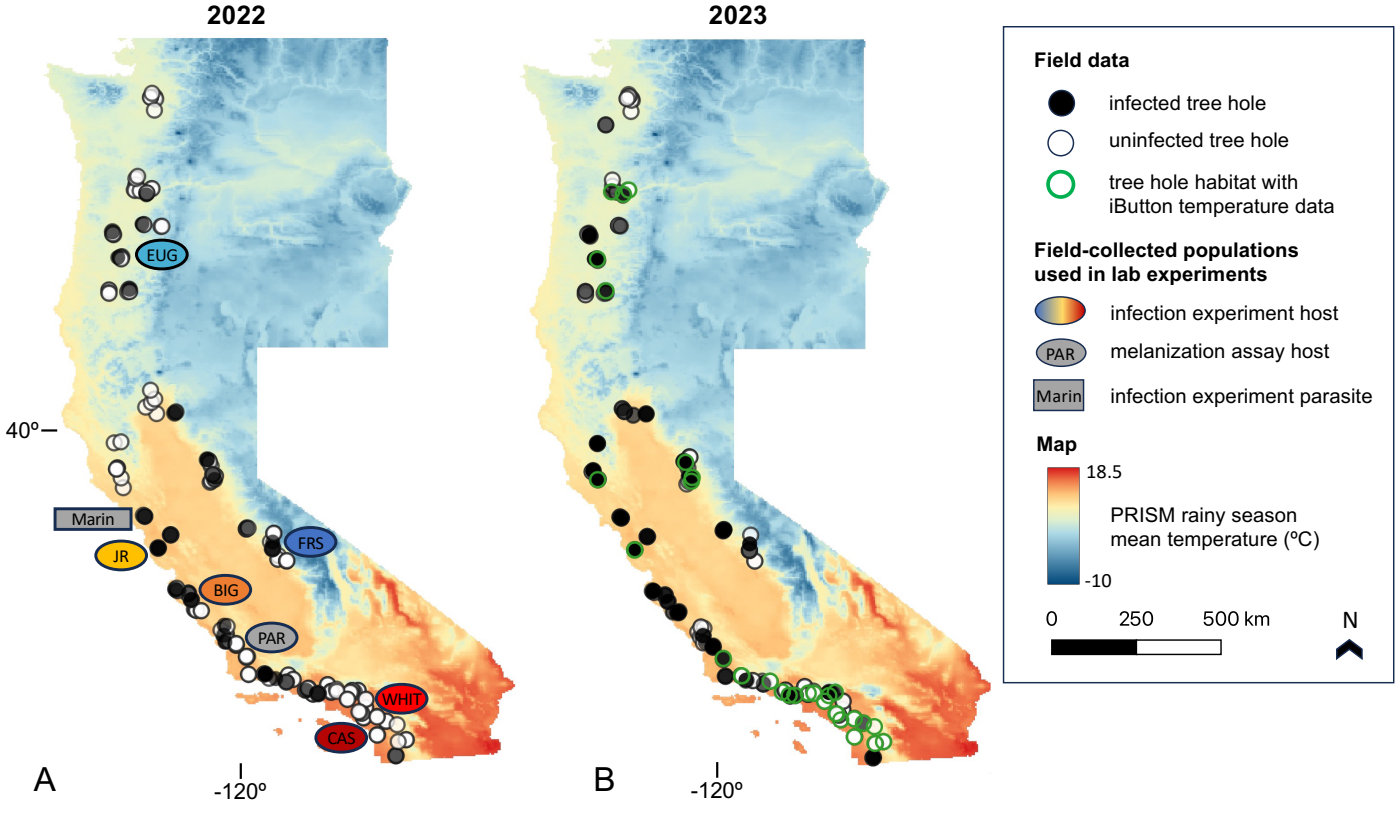
2022
2023
EUG
Marin
JR
FRS
BIG
PAR
WHIT
CAS
40°
-120°
A
B
Field data
infected tree hole
uninfected tree hole
tree hole habitat with iButton temperature data
Field-collected populations used in lab experiments
infection experiment host
melanization assay host
infection experiment parasite
Map
18.5
-10
PRISM rainy season mean temperature (°C)
0
250
500 km
N

Figure 2

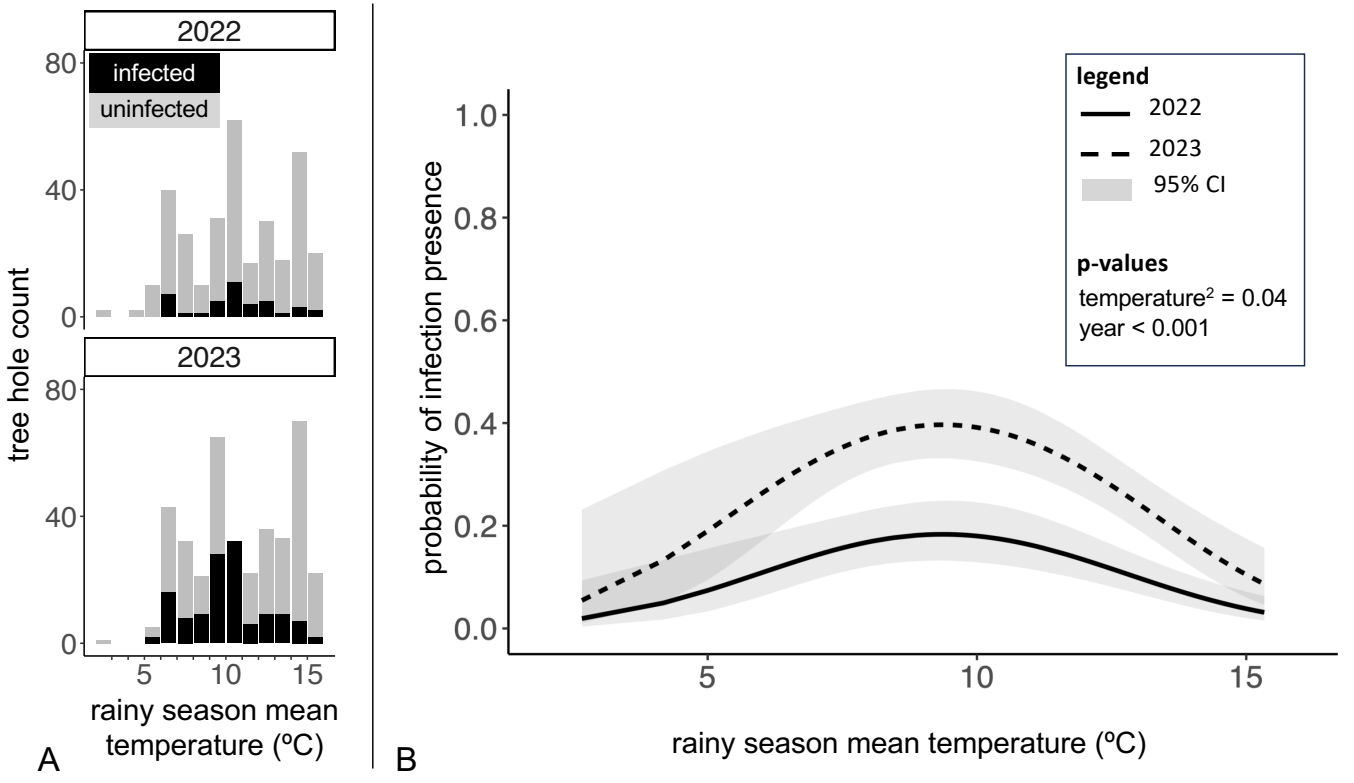
2022
infected
uninfected
2023
tree hole count
80
40
0
5
10
15
rainy season mean temperature (ºC)
A
B
probability of infection presence
1.0
0.8
0.6
0.4
0.2
0.0
legend
2022
2023
95% CI
p-values
temperature² = 0.04
year < 0.001
rainy season mean temperature (ºC)

Figure 3

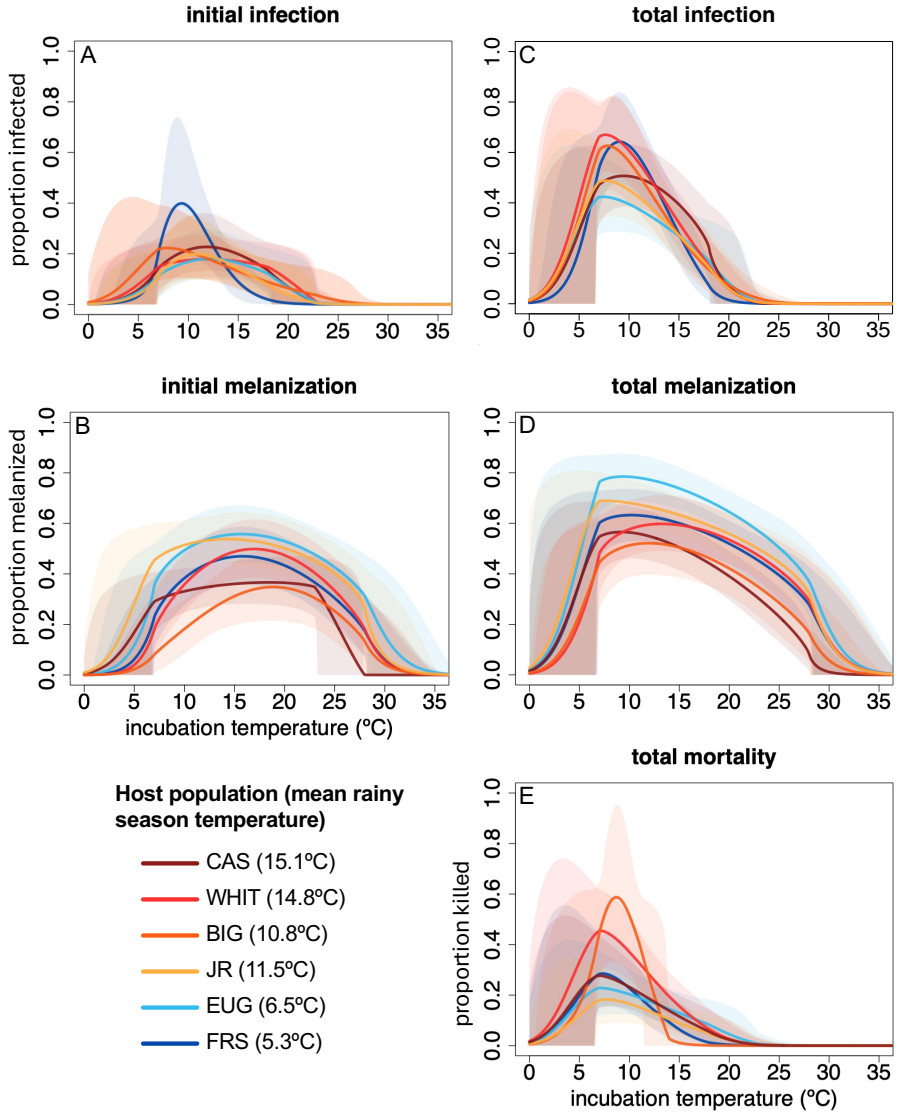
initial infection
total infection
initial melanization
total melanization
total mortality
A
B
C
D
E
proportion infected
proportion melanized
proportion killed
incubation temperature (°C)
0.0
0.2
0.4
0.6
0.8
1.0
0
5
10
15
20
25
30
35
Host population (mean rainy season temperature)
CAS (15.1°C)
WHIT (14.8°C)
BIG (10.8°C)
JR (11.5°C)
EUG (6.5°C)
FRS (5.3°C)

Figure 4

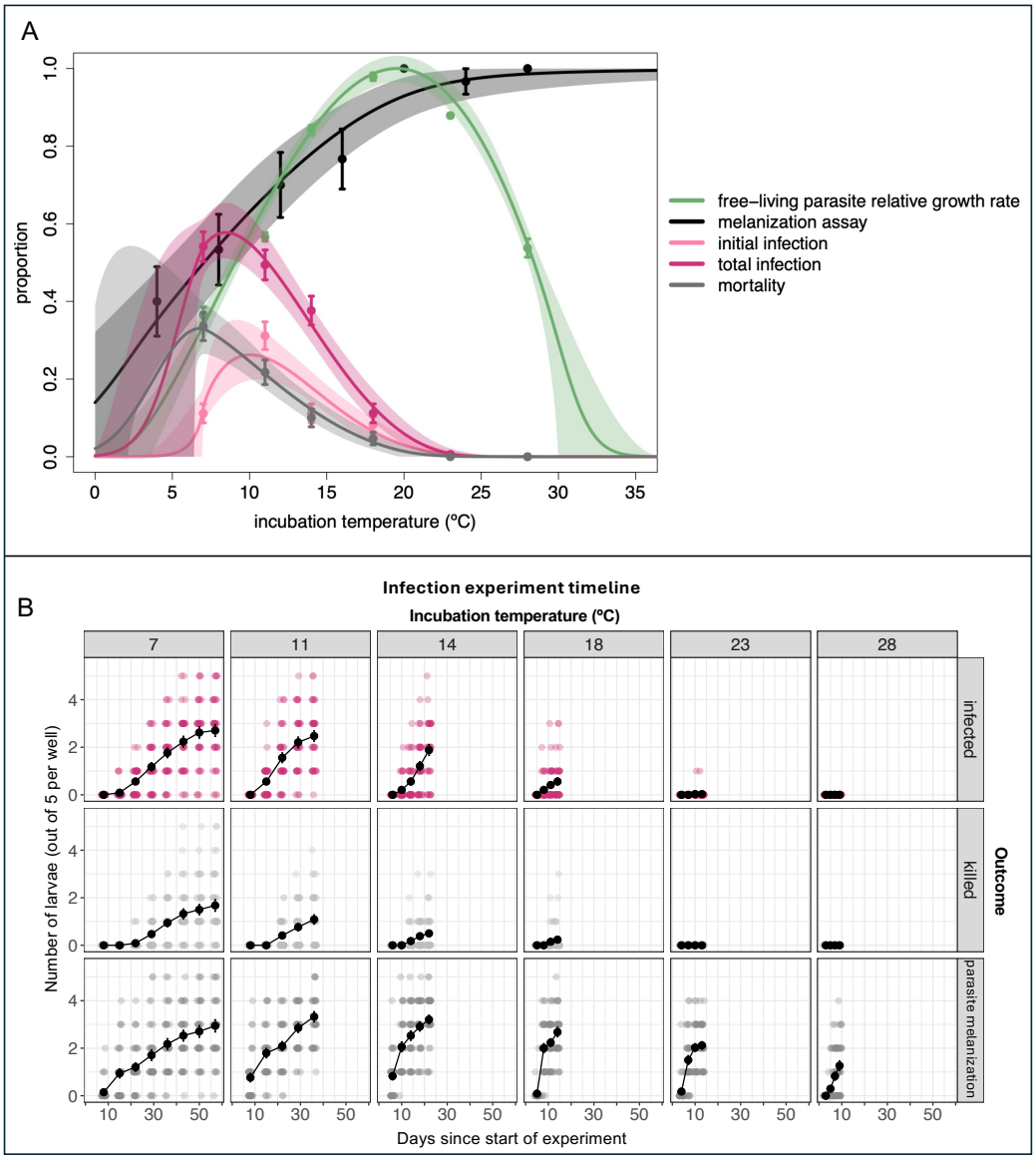
A
proportion
0.0
0.2
0.4
0.6
0.8
1.0
0
5
10
15
20
25
30
35
incubation temperature (°C)
free−living parasite relative growth rate
melanization assay
initial infection
total infection
mortality
B
Infection experiment timeline
Incubation temperature (°C)
7
11
14
18
23
28
infected
killed
parasite melanization
Outcome
Number of larvae (out of 5 per well)
0
2
4
10
30
50
Days since start of experiment